Spin Pumping and the Inverse Spin-Hall Effect via Magnetostatic Surface Spin-Wave Modes in Yttrium-Iron Garnet/Platinum Bilayers

Ieee Magnetics Letters (ISSN: 1949-307X)

Citation for the published paper:
Balinsky, M. ; Ranjbar, M. ; Haidar, M. et al. (2015) "Spin Pumping and the Inverse Spin-Hall Effect via Magnetostatic Surface Spin-Wave Modes in Yttrium-Iron Garnet/Platinum Bilayers". Ieee Magnetics Letters, vol. 6 pp. Article Number: UNSP 3000604.

http://dx.doi.org/10.1109/lmag.2015.2471276

Spin pumping and the inverse spin Hall effect via magnetostatic surface spin-wave modes in YIG/Pt bilayers

Michael Balinsky,[1] Mojtaba Ranjbar,[1] Mohammad Haidar,[1] Philipp Dürrenfeld,[1] Randy K. Dumas,[1] Sergiy Khartsev,[2] Andrei Slavin,[4] Johan Åkerman[1,3]

[1]Department of Physics, University of Gothenburg, 412 96, Gothenburg, Sweden
[2]Department of Integrated Devices and Circuits, School of ICT, Royal Institute of Technology (KTH), Electrum 229, 164 40 Kista, Sweden
[3]Materials Physics, School of ICT, Royal Institute of Technology (KTH), Electrum 229, 164 40 Kista, Sweden
[4]Department of Physics, Oakland University, Rochester, 48309, Michigan, USA

Abstract— Spin pumping at a boundary between a yttrium-iron garnet (YIG) film and a thin platinum (Pt) layer is studied under conditions in which a magnetostatic surface spin wave (MSSW, or Damon-Eshbach mode) is excited in YIG by a narrow strip-line antenna. It is shown that the voltage created by the inverse spin Hall effect (ISHE) in Pt is strongly dependent on the wavevector of the excited MSSW. For YIG film thicknesses of 41 and 0.9 microns, the maximum ISHE voltage corresponds to the maximum of efficiently excited MSSW wavevectors and does not coincide with the maximum of absorbed microwave power**.** For a thinner (0.175 um) YIG film the maximum of the ISHE voltage moves closer to the ferromagnetic resonance and almost coincides with the region of the maximum microwave absorption. We show that the observed effect is related to the change in the thickness profile and the wavenumber spectrum of the excited MSSW taking place when the YIG film thickness is increased.

Index Terms— Inverse spin Hall effect, spin pumping, a magnetostatic surface spin wave

I. INTRODUCTION

The generation and detection of pure spin currents in ferromagnetic/normal metal heterostructures has attracted much attention during the last decade in both fundamental and applied spintronics [Wang 2014, Heinrich 2011]. Pure spin currents in such heterostructures are commonly generated and detected via spin pumping [Tserkovnyak 2009, Castel 2012, Ando 2009, Qiu 2012, Ando 2008, Burrowes 2012, Hoffmann 2013] and the inverse spin Hall effect (ISHE) [Hoffmann 2013], respectively. As is shown schematically in Fig. 1(a), a precessing magnetization injects a pure spin current J_S into the adjacent normal metal [Tserkovnyak 2002]. Then, via the ISHE, J_S is converted into a transverse charge current $J_{C,}$ and a measurable transverse voltage is established in the normal metal layer. Crucial material parameters—such as the spin mixing conductance, the spin Hall angle, and the spin diffusion length—can be calculated from spin pumping and ISHE measurements [Wang 2014, Hahn 2013]. An in-depth understanding of spin pumping and the ISHE is also useful for the study of the inverse process—namely, the compensation of magnetic damping and the generation of spin waves in ferromagnets [Jungfleisch 2015, Kajiwara 2010, Demidov 2012, Kurebayashi 2011, Hamadeh 2014, Kapelrud 2013].

Layered structures consisting of a ferrimagnetic insulator $Y_3Fe_5O_{12}$ (YIG) film, which has an ultra-low magnetic damping, and a platinum (Pt) layer, which has a strong spin-orbit coupling, are ideal materials for studying both spin pumping and magnetic damping compensation [Kajiwara 2010, Hamadeh 2014, Kapelrud 2013].

Since spin pumping is an intrinsically interfacial phenomenon, it is no surprise that its efficiency would depend on the amplitude of the spin wave mode at the YIG/Pt interface. Thus, as has been shown in a number of theoretical papers [Kapelrud 2013, Zhou 2013], *exchange-dominated surface* spin-wave modes—which have exponential thickness profiles due to a strong surface anisotropy and a maximum amplitude at the YIG/Pt interface—could produce a more efficient source of pumped spins than a uniform (k=0) ferromagnetic resonance (FMR) mode. In this work, our goal is to experimentally study spin pumping in a YIG/Pt bilayer induced by a *magnetostatic surface spin wave* (MSSW or Damon–Eshbach mode [Damon 1961]) excited in the YIG film when the in-plane wavenumber, and therefore the exponential thickness profile of this mode, is varied.

In contrast with previous investigations, in which spin pumping was produced by uniform magnetization precession [Rezende 2013], backward volume magnetostatic waves (BVMSWs) [Chumak 2012], or standing surface spin waves generated in a microwave cavity having relatively small in-plane wavevectors [Sandweg 2010], our focus is on MSSWs excited by a microstrip transducer of width b=100 μm which excites a wide range of wavevectors $0<k<2\pi/b$. As will be demonstrated below, our experiments show that the MSSW with the largest effectively excited in-plane wavevectors—and therefore the most “surface-like” thickness distribution of variable magnetization—provide the most efficient spin pumping into the Pt layer and the largest ISHE voltage.

II. EXPERIMENTS

Corresponding author: johan.akerman@physics.gu.se

For our experiments, we used three YIG/Pt samples based on three YIG films grown on single-crystal $Gd_3Ga_5O_{12}$ (GGG) substrates and having different thicknesses (*S*): 41 μm, 0.9 μm, and 0.175 μm. The two thicker films (*S* = 41 μm and 0.9 μm) were grown using a liquid phase epitaxy (LPE) method [Zavislyak 2011], while the thinnest film (*S* = 0.175 μm) was grown using pulsed laser deposition (PLD) [Zavislyak 2011, Haidar 2015]. The parameters of all the YIG films are presented in Table 1. The YIG waveguides, Fig. 1(b), of length *L* = 8.4 mm and width *W* = 1 mm, were lithographically defined on the GGG substrates. The parameters of the "bare" YIG film waveguides were analyzed by measuring the absorption spectra $S_{11}(H)$ using a vector network analyzer (VNA) as a function of the applied bias magnetic field *H*. All the samples were then cleaned using a heated Piranha solution [Jungfleisch 2013] and a 6 nm thick Pt layer was deposited on the waveguides using magnetron sputtering at room temperature. Finally, a 60 nm thick layer of SiO_2 was sputtered on top of the Pt to ensure galvanic separation from the microstrip transducer.

The excitation of the MSSWs was performed by means of a microstrip transducer of width *b* = 100 μm, shorted at the ends and placed along the length of the YIG waveguide, as shown schematically in Fig. 1(b). Such a transducer can excite a reasonably wide range of wavevectors ($0<k<2\pi/b$) [Ganguly 1975, Sethares 1985] with $k_{max} \approx 2\cdot\pi/b \approx 600$ cm^{-1}, which is one order of magnitude larger than the maximum wavevector excited in the previous YIG/Pt MSSW measurements[Chumak 2012].

The bias magnetic field was directed along the length of the YIG-film waveguide, *i.e.* along the *z*-axis in Fig. 1(a, b), promoting the excitation of the quantized MSSW modes with wavevectors $k \approx k_y = (2n+1)\cdot\pi/W >> k_z$, (n = 0, 1, 2…,) determined by the width *W* of the waveguide. Such an experimental geometry allows for measurements of the spectrum of excited MSSW using a VNA in either the reflection, $S_{11}(H)$, or the transmission, $S_{12}(H)$, configuration. All the measurements of the S_{ij} parameters were performed at a fixed frequency of *f*= 5.1 GHz and a fixed input microwave power of *P* = 1.5 dBm. It should be noted that, due to the orientation of the input and output transducers along the axis of the YIG waveguide, the direct coupling between the transducers was less than -45 dB, which significantly increased the measurement sensitivity. In order to measure the dc ISHE voltage (V_{ISHE}) in the Pt layer, we used a lock-in amplifier and modulated the signal of the microwave generator with a modulation frequency of f_m = 4.32 kHz.

III. RESULTS AND DISCUSSION

The measured $S_{11}(H)$ spectra of the "bare" waveguides with the YIG films of thickness 41 μm, 0.9 μm, and 0.175 μm are shown in Fig. 2 (a), (b), and (c), respectively. The experimental spectra of the thicker LPE YIG film waveguides (*S* = 41 μm, 0.9 μm), shown in Fig. 2(a) and 2(b), contain a number of well-defined quantized MSSW peaks, the field intervals between which are determined by the width of the YIG waveguide. In the thinnest PLD YIG film sample (*S*=0.175 μm), shown in Fig. 2(c), the quantized width modes are not seen due to the much larger FMR linewidth of the PLD YIG sample (about 30 Oe compared to 1 Oe). Note that in all the spectra presented in Fig. 2 the larger bias magnetic fields correspond to the smaller MSSW wavevectors.

The field dependency of the absorption spectrum $S_{11}(H)$ and V_{ISHE} measured for YIG/Pt bilayers of YIG thickness 41 μm, 0.9 μm, and 0.175 μm and Pt thickness of 6 nm are shown in Fig. 3(a–c). Also shown are the corresponding values of the dimensionless wave number *kS* calculated for MSSW modes using the YIG film parameters presented in the Table 1 and the Damon–Eshbach dispersion relation [Damon 1961]

$$kS = -0.5\ln[(\omega_H+\omega_M/2-\omega)(\omega_H+\omega_M/2+\omega)/(\frac{\omega_M}{2})^2] \qquad (1)$$

where $\omega = 2\pi f$, $\omega_H = \gamma H$, $\omega_M = \gamma\cdot 4\pi M_0$, *H* is the external bias magnetic field, and M_0 is the saturation magnetization of YIG.

It can be seen from Fig. 3(a) and 3(b) that, in the YIG/Pt bilayers based on the high-quality LPE YIG films, the quantized MSSW width modes, clearly seen in Fig. 2(a) and 2(b), are strongly suppressed due to the additional losses induced by spin pumping into the adjacent Pt layer. It is important to note that such additional losses is generally assumed due to the effect of the spin pumping into Pt.

Using Eq. (1) and $k_{max} \approx 600$ cm^{-1}, we estimated the field ranges for the MSSW excitation in the YIG films of thickness *S* = 41 μm, 0.9 μm, and 0.175 μm to be 210 Oe, 33 Oe, and 6.4 Oe, respectively. These estimated field ranges of the MSSW excitation are in good agreement with the measured spectra for the high-quality LPE YIG films of thicknesses 41 μm and 0.9 μm, with FMR linewidths on the order of 1 Oe (see Table 1). In the thin (*S* = 0.175 μm) PLD YIG film (FMR linewidth about 30 Oe), the observed field range of the MSSW excitation of about 80 Oe is significantly larger than the calculated value of 6.4 Oe. This result is consistent with a relatively large inhomogeneous broadening that has been experimentally observed for this film using broadband FMR.

It is clear from Figures 3(a) and 3(b) that, for relatively thick LPE YIG films, the experimentally measured $S_{11}(H)$ absorption spectrum (solid line) differs significantly from the V_{ISHE} response (dots and solid line). Simply put, in the thickest (*S*=41 μm) LPE YIG film sample, the maximum of the microwave absorption in the YIG film waveguide corresponds to $kS \approx 0.14$ close to FMR, while the maximum of the voltage V_{ISHE} induced by the ISHE in the adjacent Pt layer corresponds to $kS \approx 0.54$, which is close to the maximum MSSW wavevector effectively excited by our microstrip transducer of width *b*=100 μm (note that, as the MSSW wavevector increases, the excitation efficiency of the microstrip transducer decreases as $\sin^2(kb/2)/(kb/2)^2$ [Ganguly 1975, Sethares 1985]. In fact, in both LPE YIG films (*S*=41 μm and *S*=0.9 μm), there are relatively large bias field ranges

characterized by the significant absorption of the microwave energy at small wavevectors and no observable V_{ISHE}. A significant V_{ISHE} is only found for the MSSW modes with finite and sufficiently large wavevectors. In contrast, the $S_{11}(H)$ microwave absorption spectrum measured for the thinnest (0.175 μm) PLD YIG film shows an almost perfect coincidence with V_{ISHE}, as shown in Fig. 3(c).

The surface nature of the MSSW excited in the YIG film manifests itself most strongly when there is a significant difference in the amplitude of the excited spin-wave mode at the opposite surfaces of the YIG film. In the absence of a large surface anisotropy, the ratio of the MSSW amplitude at the top (I_{top}) and bottom (I_{bottom}) surfaces of the YIG film can be expressed as $I_{top}/I_{bottom} \propto exp(2kS)$ [Damon 1961]. For the thickest YIG film (S =41 μm), shown in Fig. 3(a), at kS = 0.54, corresponding to the maximum of the V_{ISHE} response, we find I_{top}/I_{bottom} = 2.94. This means that a significant fraction of the MSSW mode energy is concentrated at the YIG/Pt interface. At the same time, a similar exercise for the LPE YIG film of thickness S=0.9 μm at kS =0.021, corresponding to the maximum of the V_{ISHE} response in this film, returns a relatively small ratio of I_{top}/I_{bottom}=1.06; this alone cannot explain the shift between the maxima of the microwave absorption and V_{ISHE} observed in Fig. 3(b). However, as explained in the literature [Kapelrud 2013, Zhou 2013, Bobkov 1993], the presence of a uniaxial surface anisotropy at the YIG film interface with Pt can lead to the concentration of the MSSW mode energy at the YIG film interface. Finally, no noticeable difference between the microwave absorption and V_{ISHE} responses could be seen for the thinnest (S=0.175 μm) YIG film, due to the very small value of $k_{max} \cdot S < 0.01$ and a practically uniform excitation profile.

In summary, we have experimentally demonstrated that, when a MSSW is excited in a YIG film, the V_{ISHE} induced by spin pumping from an adjacent YIG film to a Pt layer strongly depends on the wavevector of the excited MSSW, and takes its maximum value for the maximum MSSW wavevector effectively excited by the microwave transducer. This effect is most prominent in thick YIG films, where the surface character of the excited MSSW mode is most pronounced.

Table 1. Magnetic properties of YIG films

YIG film number	Growth method	Thickness(S) (μm)	Magnetization $4\pi M_{eff}$ (Oe)	FWHM (Oe)
1	LPE	41	1750	0.6
2	LPE	0.9	2118	1.0
3	PLD	0.175	2157	33.0

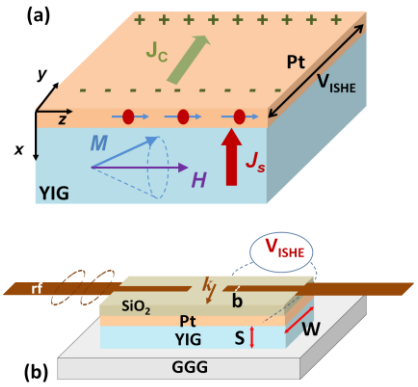

Fig. 1. (a) Magnetization precession in the YIG layer creates a transverse spin current J_s in the Pt layer. Due to the ISHE this spin current is converted into a charge current J_c, which creates a measurable ISHE voltage in Pt. (b) Schematic layout of the experimental YIG/Pt waveguide and microstrip transducer.

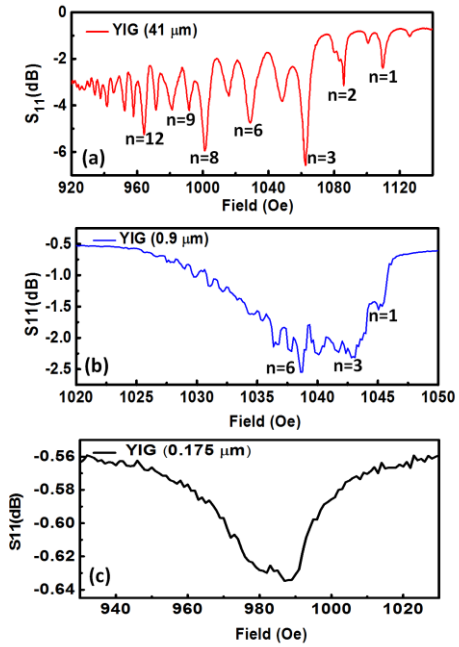

Fig. 2. Microwave absorption spectra $S_{11}(H)$ measured at a frequency of 5.1 GHz and with input microwave power of 1.5 dBm in the "bare" YIG film waveguides for S= (a) 41, (b) 0.9 and (c) 0.175 μm.

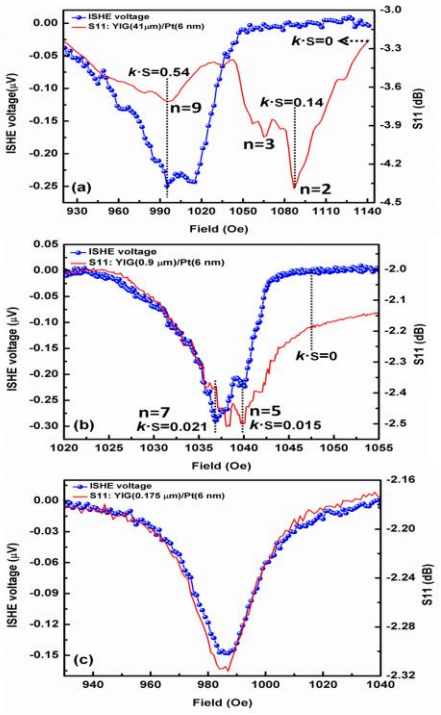

Fig. 3. Microwave absorption spectra $S_{11}(H)$ (solid lines, right axis) and the ISHE voltage V_{ISHE} (H) measured in Pt (dots connected by solid lines, left axis) as a function of the bias magnetic field H for the YIG/Pt bilayer waveguides with S= (a) 41, (b) 0.9, and (c) 0.175 μm.

ACKNOWLEDGMENT

This work was supported by the Swedish Research Council (VR), the Swedish Foundation for Strategic Research (SSF), and the Knut and Alice Wallenberg Foundation. This work was also supported by the European Research Council (ERC) under the European Community's Seventh Framework Programme (FP/2007-2013)/ERC Grant 307144 "MUSTANG." Supported in part by grants DMR-1015175 and EPMD-1305574 from the US National Science Foundation, by contracts from the US Army TARDEC and RDECOM, and by DARPA MTO/MESO grant No. 66001-11-1-4114 are also gratefully acknowledged.

REFERENCES

Ando K, Takahashi S, Harii K, Sasage K, Ieda J, Maekawa S, and Saitoh E (2008), "Electric Manipulation of Spin Relaxation Using the Spin Hall Effect", *Phys. Rev. Lett.,* vol. 101, pp. 036601.

Ando K, Ieda J, Sasage K, Takahashi S, Maekawa S, and Saitoh E (2009), "Electric detection of spin wave resonance using inverse spin-Hall effect", *Appl. Phys. Lett.,* vol. 94, pp. 262505.

Burrowes C, Heinrich B, Kardasz B, Montoya EA, Girt E, Sun Y, Song YY, Wu M (2012), "Enhanced spin pumping at yttrium iron garnet/Au interfaces", *Appl. Phys. Lett.,* vol. 100, pp. 092403.

Bobkov VB, Zavislyak IV (1993), "Electromagnetic waves in anisotropic multilayer ferrite structure with trigonal symmetry under parallel magnetization", *Phys. Stat. Sol. (b),* vol. 176, pp. 227.

Castel V, Vlietstra N, Wees BJ, Youssef JB (2012), "Frequency and power dependence of spin-current emission by spin pumping in a thin film YIG/Pt system", *Phys. Rev. B*, vol. 86, pp. 134419.

Chumak AV, Serga A A, Jungfleisch MB, Neb R, Bozhko DA, Tiberkevich VS, and Hillebrands B (2012), "Direct detection of magnon spin transport by the inverse spin Hall effect", *Appl. Phys. Lett.,* vol 100, pp. 082405.

Demidov V, Urazhdin S, Ulrichs H, Tiberkevich V, Slavin A, Baither D, Schmitz G, Demokritov S (2012), "Magnetic nano-oscillator driven by pure spin current", *Nature Materials*, vol. 11, pp. 1028.

Damon RW, and Eshbach JR (1961), "Magnetostatic modes of a ferromagnet slab", *J. Phys. Chem. Solids,* vol. 19, pp.308.

Ganguly AK, and Webb DC (1975), "Microstrip excitation of magneto-static surface waves", *IEEE Trans. MTT,* vol. 23, pp. 998.

Heinrich B, Burrowes C, Montoya E, Kardasz B, Girt E, Song Y-Y, Sun Y, and M Wu (2011), "Spin Pumping at the Magnetic Insulator (YIG)/Normal Metal (Au) Interfaces", *Phys. Rev. Lett.,* vol. 107, pp. 066604.

Harii K, An T, Kajiwara Y, Ando K, Nakayama H, Yoshino T, and Saitoh E (2011), "Frequency dependence of spin pumping in Pt/Y3Fe5O12 Film", *J. Appl. Phys.,* vol. 109, 116105.

Hahn C, Loubens G de, Klein O, Viret M, Naletov VV, and Ben Youssef J (2013), "Comparative measurements of inverse spin Hall effects and magnetoresistance in YIG/Pt and YIG/Ta", *Phys. Rev. B*, vol. 87, pp.174417.

Hoffmann A (2013), "Spin Hall Effects in Metals", *IEEE Trans. Magn.,* vol. 49, pp. 5172.

Hamadeh A, D'Allivy Kelly O, Hahn C, Meley H, Bernard R, Molpeceres AH, Naletov VV, Viret M, Anane A, Cros V, Demokritov SO, Prieto JL, Muñoz M, De Loubens G, and Klein O (2014), "Full Control of the Spin-Wave Damping in a Magnetic Insulator Using Spin-Orbit Torque",*Phys. Rev. Lett.,* vol. 113, pp.197203.

Haidar M, Ranjbar M, Balinsky M, Dumas RK, Khartsev S, and Åkerman J (2015), "Thickness and temperature dependent magnetodynamic properties of YIG thin films", *J. Appl. Phys.,* vol. 117, pp. 17D119.

Jungfleisch MB, Lauer V, Neb R, Chumak AV, Hillebrands B (2013), "Improvement of the yttrium iron garnet/platinum interface for spin pumping-based applications", *Appl. Phys. Lett.,* vol. 103, 022411.

Jungfleisch MB, Chumak AV, Kehlberger A, Lauer V, Kim DH, Onbasli MC, Ross CA, Kläui M, and Hillebrands B (2015), "Thickness and power dependence of the spin-pumping effect in Y3Fe5O12/Pt heterostructures measured by the inverse spin Hall effect", *Phys. Rev. B*, vol. 91, pp. 134407.

Kajiwara Y, Harii K, Takahashi S, Ohe J, Uchida K, Mizuguchi M, Umezawa H, Kawai H, Ando K, Takanashi K, Maekawa S, and Saitoh E(2010), "Transmission of electrical signals by spin-wave interconversion in a magnetic insulator", *Nature*, vol. 464, pp. 262.

Kurebayashi H, Dzyapko O, Demidov VE, Fang D, Ferguson AJ, and Demokritov SO (2011), "Controlled enhancement of spin current emission by three-magnon splitting", *Nature Materials,* vol. 10, pp. 660.

Kapelrud A, and Brataas A (2013), "Spin Pumping and Enhanced Gilbert Damping in Thin Magnetic Insulator Films", *Phys. Rev. Lett., v*ol. 111, pp. 097602.

Qiu Z, Kajiwara Y, Ando K, Fujikawa Y, Uchida K, Tashiro T, Harii K, Yoshino T, Saitoh E (2012), "All-oxide system for spin pumping", *Appl. Phys. Lett.,* vol. 100, pp. 022402.

Rezende SM, Rodriguez-Suarez RL, Soares MM, Vilela-Leao LH, Ley Dominguez D, and Azevedo A (2013), "Enhanced spin pumping damping in yttrium iron garnet/Pt bilayers", *Appl. Phys. Lett*., vol. 102, pp. 012402.

Sethares JC, Weinberg IJ (1985), "Theory of MSW transducers", *Circuits Systems Signal Proc.,* vol 4, pp. 41.

Sandweg CW, Kajiwara Y, Ando K, Saitoh E, and Hillebrands B (2010), "Enhancement of the spin pumping efficiency by spin wave mode selection", *Appl. Phys. Lett.,* vol. 97, 252504.

Sun Y, Chang H, Kabatek M, Song YY, Wang Z, Jantz M, Schneider W, Wu M, Montoya E, Kardasz B (2013), "Damping in yttrium iron garnet nanoscale films capped by platinum", *Phys. Rev. Lett.,* vol 111, 106601.

Tserkovnyak Y, Brataas A, and Bauer GEW (2002), "Enhanced Gilbert damping in thin ferromagnetic films", *Phys. Rev. Lett.,* vol. 88, pp.117601.

Wang H, Du C, Hammel PC, and Yang F (2014), "Spin Current and Inverse Anomalous Hall Effect in Ferromagnetic metals Probed by $Y_3Fe_5O_{12}$-Based Spin Pumping", *Appl. Phys. Lett.,* vol. 104, pp. 202405.

Wang HL, Du CH, Pu Y, Adur R, Hammel PC, Yang FY (2014), “Scaling of Spin Hall Angle in 3d, 4d, and 5d Metals from Y3Fe5O12/Metal Spin Pumping”, *Phys. Rev. Lett.,* vol. 112, pp. 197201.

Zychowicz T, Krupka J (2006), “Measurements of conductivity of thin metal films at microwave frequencies”, *Proc. of SPIE*, vol. 6159, 61591X.

Zavislyak IV, Popov MA (2011), “Microwave Properties and Application of Yttrium Iron Garnet (YIG) Films: Current State of ART and Perspectives”, *in: Yttrium: Compounds, Production and Applications, Editor: B.D. Volkerts, Nova Science Publishers, Inc.,* Chapter 3, pp.87–125.

Zhou Y, Jiao HJ, Chen Y, Bauer GEW, and Jiang X (2013), “Current-induced spin-wave excitation in Pt/YIG bilayer”, *Phys. Rev. B,* vol 88, pp. 184403.